From Gibbs- To Langmuir-Type Adsorbed Layers: Alkylated Azacrown Ethers At Liquid-Liquid Interfaces

ARTICLE *in* THE JOURNAL OF PHYSICAL CHEMISTRY C · JUNE 2012

Impact Factor: 4.77 · DOI: 10.1021/jp3017985

THE JOURNAL OF PHYSICAL CHEMISTRY C

Article

pubs.acs.org/JPCC

From Gibbs- To Langmuir-Type Adsorbed Layers: Alkylated Azacrown Ethers At Liquid−Liquid Interfaces

K. Wojciechowski* and A. Brzozowska†

Faculty of Chemistry, Warsaw University of Technology, Noakowskiego 3, 00-664 Warsaw, Poland

ABSTRACT: Adsorption properties of three alkylated diazacrown ether derivatives in a toluene−water system are described. The three derivatives share the same hydrophilic diaza-18-crown-6 moiety, substituted at both nitrogen atoms with decyl (ACE-10), hexadecyl (ACE-16), or tetracosane (ACE-24) alkyl chains. Dynamic interfacial tension measurements at the toluene−water interface revealed a nondiffusional mechanism of adsorption for all three ACEs. The interfacial tension isotherms obtained from the drop-shape analysis were fitted with a reorientation model (for ACE-10 and ACE-16) and Langmuir model (ACE-24), pointing to different structures of the respective spontaneously adsorbed layers: loose (Gibbs-like) for the short-chain derivatives and dense (Langmuir-like) for the long-chain. These results are in full agreement with previous neutron and X-ray reflectivity studies. Despite an apparent cmc, the ACE molecules probably do not form reverse micelles in highly concentrated solutions in nonpolar solvents.

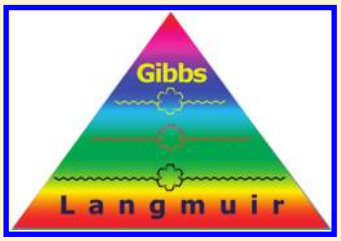

INTRODUCTION

The alkylated azacrown ethers (ACE) possess two structural features, which make them especially useful for interfacial transport purposes: lipophilic alkyl chains and hydrophilic macrocyclic cavity. The latter is provided by the nitrogen and oxygen atoms present in the crown ether moiety and brings in the cation-coordinating ability. The selectivity of ion recognition depends on the number and distribution of nitrogen and oxygen atoms in the cavity. For example a six-oxygen 18-crown-6 ether selectively complexes K^+, Sr^{2+}, and Ba^{2+} ions,[1] while its four-nitrogen analogue (cyclam) is most selective to Ni(II) and Cu(II).[2] The mixed nitrogen−oxygen azacrown ethers, e.g., diaza-18-crown-6 ether in polar solvents display the highest selectivity toward Ag^+, Cu^{2+}, Cd^{2+}, and Pb^{2+}. Alkylation of the nitrogen atoms does not alter significantly their complexation selectivity.[3]

The amphiphilic nature of ACE, being a direct consequence of their structure, plays a crucial role in their ability to transport ions between two immiscible solutions, e.g., in liquid−liquid extractions. The didecyl substituted ACE (ACE-10, see Figure 1) has been extensively used by the group of J. Buffle as Cu(II) and Pb(II) cocarrier in permeation liquid membranes (PLM) for environmental speciation studies.[4] Even though the role of adsorption in extraction processes in general is still not clear, for extractants with pronounced amphiphilic properties, it is believed to be decisive.[5] We have shown previously for ACE-10 that its interfacial properties determine the overall selectivity of Cu(II) transport through the PLM. In a typical PLM experiment, ACE-10 is dissolved together with the fatty acid in an organic membrane. While the fatty acid transports Cu(II) ions through the bulk of the membrane, ACE-10 ensures the interfacial transfer of metal ions from the aqueous to the membrane phase. Thanks to its surface activity combined with unique complexing abilities, ACE-10 is capable of attracting both Cu(II) ions and fatty acid molecules to the interfacial region, where a dimeric Cu(II)-fatty acid complex is formed and further transported through the membrane. Hence, ACE-10 effectively plays a role of phase transfer catalyst for Cu(II) ions.[6]

Since not only adsorption but also several other chemical processes may take place in the interfacial layer at the liquid−liquid interface, the structure of this layer is of paramount importance. In this article, we explore the question of the influence of the length of the lipophilic part of ACE on the structure of the interfacial layer at a liquid−liquid interface simulating the membrane-aqueous interface in PLM. For this purpose, the surface activity of three homologous diaza-18-crown-6 with different alkyl chain lengths, $-C_{10}H_{21}$, $-C_{16}H_{33}$, nd $-C_{24}H_{49}$ (Figure 1), at the toluene−water interface will be compared.

EXPERIMENTAL SECTION

Chemicals. *N,N′*-Didecyldiaza-18-crown-6 ether (ACE-10) was obtained from Merck (Kryptofix 22DD). *N,N′*-Dihexadecyl-4,13-diaza-18-crown-6 (ACE-16) and *N,N′*- ditetracosane-4,13-diaza-18-crown-6 (ACE-24) were prepared as described in ref 7. Freshly deionized water from a Millipore Simplicity UV system (18.2×10^6 Ω cm, irradiated with UV lamp) was used for the measurements. Toluene (puriss. p.a. ACS reagent for UV spectroscopy) was purchased from Fluka and purified by liquid−liquid extraction with water. Its surface purity was checked prior to preparation of each new solution by measuring the dynamic interfacial tension against water for 1 h.

Measurements. The dynamic interfacial tension measurements ($\gamma(t)$) were performed using drop profile analysis tensiometers: PAT-1 (SINTERFACE Technologies, Germany) and CAM 200 (KSV, Finland). All glassware was cleaned with

Received: February 23, 2012
Revised: April 25, 2012
Published: May 14, 2012

   dx.doi.org/10.1021/jp3017985 | J. Phys. Chem. C 2012, 116, 12584−12590

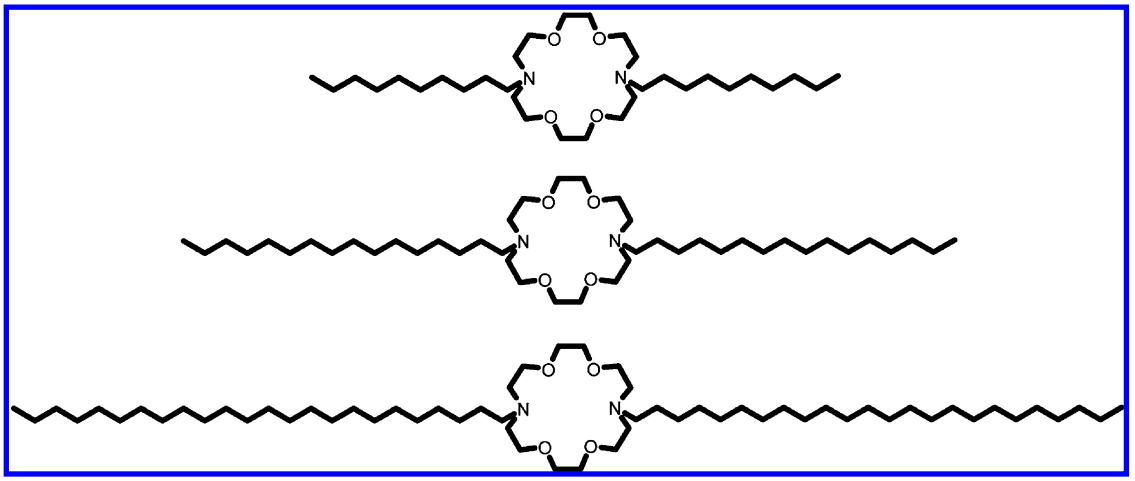

Figure 1. Structures of alkylated azacrown ethers used in the present study: ACE-10, ACE-16, ACE-24.

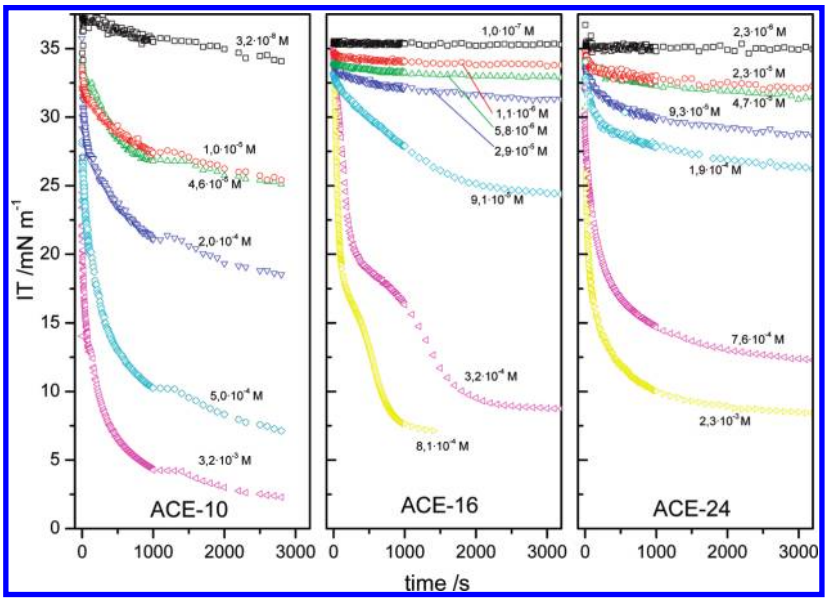

Figure 2. Dynamic interfacial tensions decays for the toluene solutions of ACE-10 (3.2×10^{-8} M, 1.0×10^{-5} M, 4.6×10^{-5} M, 2.0×10^{-4} M, 5.0×10^{-4} M, and 3.2×10^{-3} M), ACE-16 (1.0×10^{-7} M, 1.1×10^{-6} M, 5.8×10^{-6} M, 2.9×10^{-5} M, 9.1×10^{-5} M, 3.2×10^{-4} M, and 8.1×10^{-4} M) and ACE-24 (2.3×10^{-6} M, 2.3×10^{-5} M, 4.7×10^{-5} M, 9.3×10^{-5} M, 1.9×10^{-4} M, 7.6×10^{-4} M, and 2.3×10^{-3} M) at the toluene–water interface (21 °C).

acetone and Hellmanex II solution (Hellma Worldwide) and subsequently rinsed with copious amounts of Millipore water. All the experiments were performed at constant temperature (21 °C) controlled with a thermostatic bath. For $\gamma(t)$ measurements, the drop of pure water (7–36 mm^3) was formed at the tip of a steel capillary immersed in a glass cuvette (20 cm^3). The alkylated azacrown ethers (ACE-10, ACE-16, and ACE-24) were dissolved in a water-saturated toluene. All experiments were performed during at least 1 h and repeated at least three times. The equilibrium interfacial tension values were calculated from a long-time extrapolation of dynamic interfacial tension using the asymptotic solution to the Ward–Tordai equation (valid for $t \rightarrow \infty$)[8]

$$\gamma_{eq} = \gamma - \frac{RT\Gamma^2}{c_0}\sqrt{\frac{\pi}{4Dt}} \quad (1)$$

where γ is the actual value of interfacial tension, γ_{eq} the equilibrium interfacial tension, R the gas constant, T the temperature, D the diffusion coefficient, t time, and c_0 the bulk concentration of ACE.

The dynamic interfacial tension data were plotted in γ vs $t^{-1/2}$ coordinates, and the intercept with the ordinate gave the equilibrium interfacial tension, γ_{eq}. However, it should be borne in mind that, for $t \rightarrow \infty$, the effect of even minute amounts of surface-active contaminants becomes significant.[8] Therefore, in this work, only the data points below 3000 s were taken for the extrapolation, although the interfacial tension continued to decrease after this time, even for the highest concentrations. For interfacial tension data analysis, IsoFit and WardTordai software by Aksenenko were used.[9,10]

RESULTS

Dynamic Interfacial Tension. The interfacial tension decays ($\gamma(t)$) at the toluene–water interface for three homologous azacrown ethers (ACE-10, ACE-16, and ACE-24) are collected in Figure 2. In all cases, the kinetics of adsorption is much slower than expected from the diffusion-

dx.doi.org/10.1021/jp3017985 | J. Phys. Chem. C 2012, 116, 12584–12590

limited transport of alkylated azacrown ether molecules. The characteristic time for a diffusion-limited adsorption, τ_D, at bulk concentrations corresponding to the maximum surface concentration of $\Gamma = 4 \times 10^{-6}$ mol·m^{-2} ($c \rightarrow 10^{-3}$ M) and diffusion coefficient ($D = 8 \times 10^{-10}$ m^2·s^{-1}, as measured for ACE-10 with DOSY ^{1}H NMR)

$$\tau_D \approx (\Gamma/c)^2 D^{-1}$$

is of the order of seconds. For the sake of illustration, a comparison between the experimental and theoretical (calculated using Ward–Tordai equation with Langmuir equation as a boundary condition) $\gamma(t)$ decay for 10^{-4} M ACE-10 solution in toluene is shown in Figure 3.

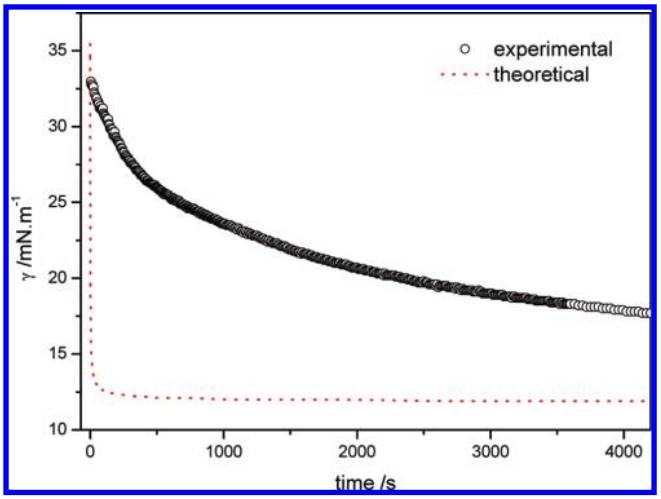

Figure 3. Comparison of experimental and theoretical (Ward–Tordai–Langmuir equation) dynamic interfacial tension decay for 10^{-4} M ACE-10 at the toluene–water interface.

The $\gamma(t)$ curves shown in Figure 2 do not reach the equilibrium values on the time scale of our measurements (one hour) even at the highest ACE concentrations. One may argue that this slow kinetics of interfacial tension decay could be a result of partitioning of ACE between the toluene and the aqueous phases. If it were the case, however, the effect should diminish with decreasing water-solubility, i.e., with an increase of the alkyl chain length.

The $\gamma(t)$ curves for short-chain ACEs (ACE-10 and ACE-16) display characteristic inflection points, especially pronounced for ACE-16. Their shape resembles that observed for surfactant mixtures, where one surface-active component quickly adsorbing to the interface is being replaced by the other, more surface-active but slower in reaching the interface. Nevertheless, similar curves have been observed, e.g., for surfactants undergoing phase transitions, and the shape of the curves alone does not have to imply the presence of surface-active impurities (see below). The decays in the first kinetic regime for both derivatives seem to be faster than in the second one. In contrast, dynamic interfacial tension curves for the longest chain derivative ACE-24 do not show any features.

Interfacial Tension Isotherms. The equilibrium values of interfacial tension as a function of logarithm of ACE concentration (i.e., interfacial tension isotherms) obtained from the long-time extrapolation of the dynamic decays are shown in Figure 4 for all three ACEs. The most pronounced differences between the three isotherms can be noticed in the low concentration region, below 10^{-4} M. For ACE-10 and ACE-16, the shape of the isotherm precludes data interpretation with simple adsorption models. Only the isotherm for the longest-chain derivative ACE-24 could be satisfactorily fitted using the Langmuir model (Table 1). Interestingly, the area per molecule in ACE-24 is very low (43 Å^2) and the same as that in the compressed state of ACE-10 and ACE-16 (see below).

The equilibrium interfacial tension data for ACE-10 and ACE-16 could be analyzed with simple models only by considering the two regions of the isotherm separately, using, e.g., two Langmuir isotherms for each region. In this work, however, the approach employed earlier for interpretation of the ACE-10 isotherm, i.e., the reorientation model, will be used. The model has been described in detail elsewhere,[11] below only an outline is given.

The basic assumption of the reorientation model is the coexistence of two distinct modes of adsorption for the same molecule. For anisotropic molecules, this may correspond to adsorption of the same molecule in two different conformations, characterized by different surface affinities (b_i) and different areas per molecule (ω_i). The model can be regarded as a simplified (two-state) version of the continuous state model for proteins with a continuous change of the adsorbing molecule orientation.[12]

The two modes of adsorption are characterized by the corresponding areas per molecule ($\omega_{exp} > \omega_{com}$). At low concentration, the higher area per molecule dominates (expanded state), and with increasing surface concentration, a transition into the state of lower area per molecule (compressed state) is observed. The ratio of surface concentrations in the two states is expressed by the surface equivalent of the principle of Braun–Le Chatelier formulated by Joos and Serrien[13]

$$\frac{\Gamma_{exp}}{\Gamma_{com}} = \beta \exp\left[\frac{\Pi(\omega_{com} - \omega_{exp})}{RT}\right] \quad (2)$$

where Γ is the surface concentration, ω is the area per molecule, the subscripts exp and com depict the expanded and compressed states, respectively, Π is the surface pressure, $\beta = (\omega_{exp}/\omega_{com})^{\alpha} \times \exp((\omega_{exp} - \omega_{com})/\omega_{\Sigma})$, ω_{Σ} is the average molar area of the components, and α is a parameter related to surface activities of the two states through the following equation:[14]

$$b_{exp}/b_{com} = (\omega_{exp}/\omega_{com})^{a} \quad (3)$$

Here, b_{exp} and b_{com} are the adsorption equilibrium constants for the expanded and compressed states, respectively. The parameter α can be interpreted as a measure of the ratio of the adsorption constants of the expanded state with respect to the compressed one. For the full set of equations, the reader is referred to the original works.[11,15–19]

The interfacial tension isotherms of both ACE-10 and ACE-16 can be well fitted using the reorientation model. The best-fit parameters are given in Table 1, and the corresponding adsorption isotherms showing surface concentrations in both states, as well as total surface concentrations are shown in Figure 4 (bottom). The area per molecule in the high surface pressure compressed state (ω_{com}) is the same for both ACE-10 and ACE-16. Only the area per molecule in the expanded state (ω_{exp}) distinguishes the two derivatives. A similar trend of increasing ω_{exp} with an increase of the alkyl chain length (C_n) have been observed for oxyethylated alcohols (C_nEO_8) sharing

dx.doi.org/10.1021/jp3017985 | J. Phys. Chem. C 2012, 116, 12584–12590

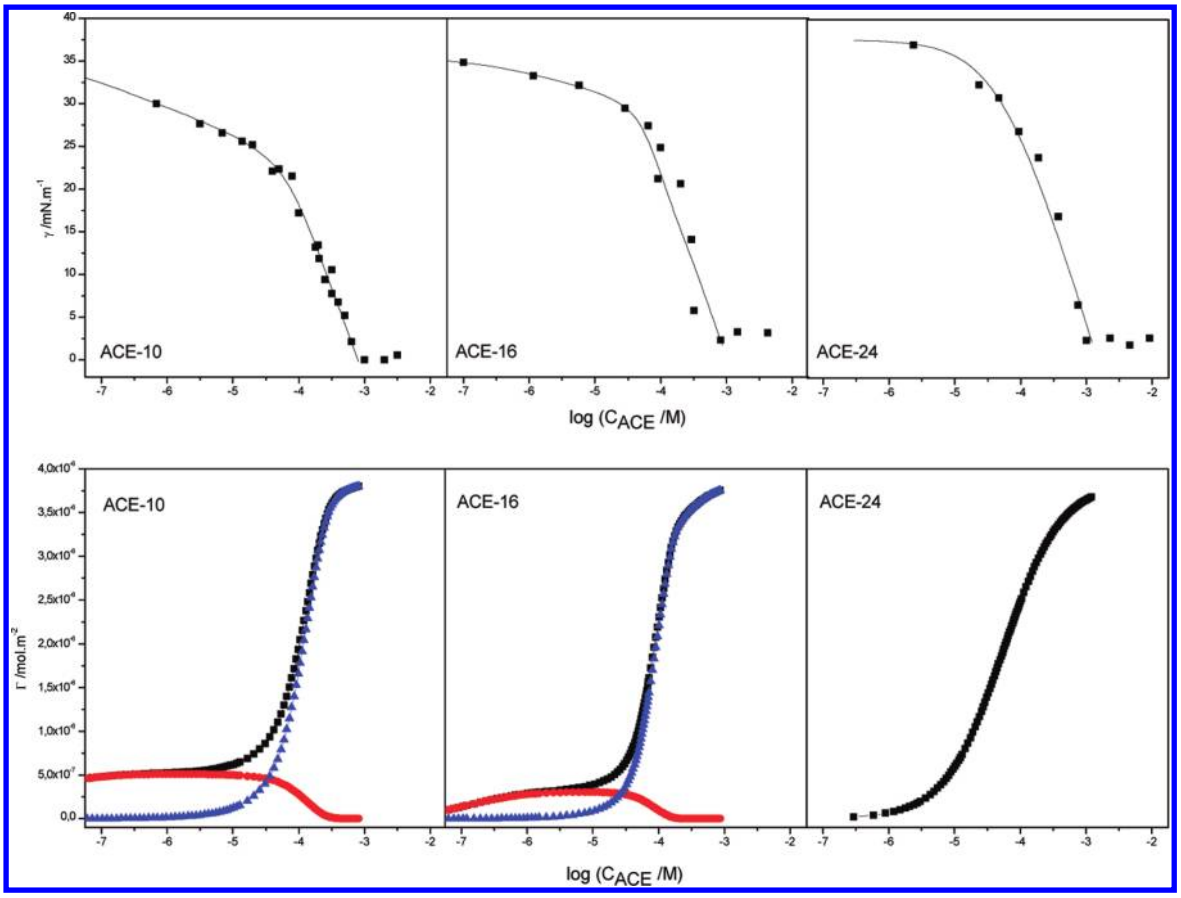

Figure 4. Interfacial tension (top) and adsorption (bottom) isotherms for ACE-10, ACE-16, and ACE-24 at the toluene−water interface (21 °C). For ACE-10 and ACE-16, two adsorbed amounts in the expanded (red circle) and compressed (blue triangle) states are given, together with the total adsorbed amount (black square).

Table 1. Best-Fit Parameters for Reorientation and Langmuir Models Applied to the Interfacial Tension Isotherms of the ACEs Used in This Study

azacrown ether	adsorption model	ω (m^2 mol^{-1})	area per molecule (Å^2)	b (m^3 mol^{-1})	$\alpha_{reorient}$
ACE-10	reorientation	$\omega_{exp} = 1.94 \times 10^6$	322	5.33×10^1	3.45
		$\omega_{com} = 2.57 \times 10^5$	43		
ACE-16	reorientation	$\omega_{exp} = 3.16 \times 10^6$	525	3.2×10^4	1.80
		$\omega_{com} = 2.57 \times 10^5$	43		
ACE-24	Langmuir	$\omega_{Langmuir} = 2.6 \times 10^5$	43	1.81×10^{-1}	

the same hydrophilic group (EO_8).[20] Unfortunately, the adsorption constants, b, for the studied ACE cannot be directly compared since, for the reorientation model, they represent the averages weighted over all surface pressures.

The high values of α (3.45 for ACE-10 and 1.80 for ACE-16) in conjunction with large differences in ω_{exp} and ω_{com} point to huge differences in surface activities for the two adsorption modes of the two short-chain ACEs. Nevertheless, a clear decreasing trend for α is seen for increasing alkyl chain length. As a result, the expanded state is getting less and less populated and eventually disappears for ACE-24, where only one adsorption state can be detected, with $\omega_{Langmuir} = \omega_{com}$. The interfacial tension isotherm for ACE-24 shown in Figure 4 (right panel) does not feature the low concentration branch with finite slope, characteristic for a two-mode adsorption behavior described by the reorientation model. While the latter could be successfully employed for the other two ACEs, for ACE-24, it does not produce any reasonable fits. As a consequence, the data for ACE-24 could be fitted to the simple Langmuir model (Table 1).

The drops of interfacial tension shown in Figure 4 suggest the existence of critical micellar concentration (cmc) for all three ACE derivatives. It is, however, striking that the interfacial tension values measured at and above these concentrations are very low (few mN/m). Given the specificity of the drop-shape analysis method, these very low values corresponding to large deformations of the toluene drop in the gravitational field are not fully reliable. Hence, an exact determination of cmc values is not possible. For this reason, despite the clear plateau on the interfacial tension isotherm shown in Figure 4, the existence of real cmc is disputable. The question of the solution behavior of ACEs, and their possible reverse hydrotropes (lipotropic) properties will be addressed in a separate article.

DISCUSSION

In our previous paper, we have shown that adsorption of the shortest-chain derivative, ACE-10, is not diffusion-limited but

dx.doi.org/10.1021/jp3017985 | J. Phys. Chem. C 2012, 116, 12584−12590

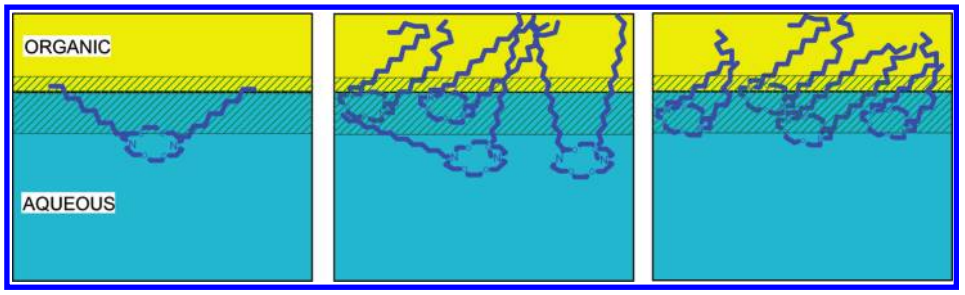

Figure 5. Schematic representation of the three possible adsorption states for the alkylated azacrown ethers at the organic−aqueous interface: expanded state (left, available for ACE-10 and ACE-16) and compressed states (middle, available for ACE-10 and ACE-16; right, available only for ACE-24).

rather seems to be related to a slow reorganization of the interfacial layer.[21] In fact, fitting of the dynamic interfacial tension curves for the studied ACEs at neutral pH with the Ward−Tordai equation (i.e., assuming diffusion-limited adsorption) would require taking assumption that either the diffusion coefficient, D, is two to three orders of magnitude smaller than expected or that the samples contain up to 10% surface-active impurities. The latter hypothesis can be excluded on the basis of an extensive ^{1}H NMR analysis in a wide range of concentrations (4.0×10^{-5} M−6.0×10^{-2} M; not shown). However, lowering the pH or increasing salt concentration significantly accelerates the interfacial tension decays for ACE-10, and the dynamic curves at low pH/high ionic strengths could be successfully fitted using reasonable sets of D, without any indication of surface-active impurities. This has lead us to the conclusion that the slow rearrangements could be related to coordination of cations (metal ions or protons, depending on the composition of the aqueous phase).[21] Since the ACE-16 and ACE-24 derivatives possess the same binding site as ACE-10 (i.e., diaza-18-crown-6 ether moiety), one may expect that the origin of the slow decay of the interfacial tension for all ACEs described in this work is similar and related mostly to chemical processes dependent on the nature of the azacrown ether headgroup, rather than the alkyl parts (see below).

The detailed analysis of interfacial tension isotherm for ACE-10 has been described in ref 22. In brief, the area per molecule in the expanded state has been assigned to the ACE-10 molecule with alkyl chains and the azacrown ring located in the plane of the interface. Using the empirical relationships for the volume and length of the all-trans alkyl chains,[23] the area per molecule in this state has been estimated to vary between 196 and 303 Å^2, of which 50−157 Å^2 would come from the azacrown ether headgroup contribution, and 2×73 Å^2 from the area per two n-decane chains. This value is in reasonable agreement with that obtained from the best-fit of the experimental data (322 Å^2). The compressed state for ACE-10 would correspond to a densely packed state, with the alkyl chains tilted with respect to the interfacial plane, and/or more than one layer of ACE-10 in the interfacial region, given a very low area per molecule (43 Å^2). This value is even smaller than the smallest value found in the literature for a single diaza-18-crown-6 ether headgroup:[24] 50 Å^2.

For ACE-16, the area per molecule in the compressed state is the same as that for ACE-10, indicating that the structures of the interfacial layer at high surface pressures are similar for the two derivatives. However, the area per molecule in the expanded state, ω_{exp}, is much higher for ACE-16 than for ACE-10. Employing the same assignment as for the shorter ACE-10 derivative, this increase of area per molecule in the expanded state would stem from the 12 additional methylene units ($2 \times C_6H_{12}$) in the alkyl chains of ACE-16. These 12 methylene units would require about 160 Å^2 when stretched in the interface plane. Thus, the corresponding estimated area per molecule in the expanded state (356−463 Å^2) corresponds reasonably well to that found from the best-fit of the interfacial tension isotherm (525 Å^2, Table 1).

In both ACE-10 and ACE-16, the expanded state has higher surface activity than the high-surface pressure state ($\alpha > 0$; $\omega_{exp}/\omega_{com} \gg 1$), although this difference decreases with an increase of the alkyl chain length. The trend of decreasing α parameter with increasing the alkyl chain length reflects the decreasing surface activity of the expanded state with respect to the compressed one. Note that, in the expanded state, as pictured schematically in Figure 5, the alkyl chains are partially exposed to the water phase, which is energetically not favorable, especially for longer alkyl chains. Apparently, for ACE-24, such a state would be so weakly surface active (large area of contact between the two lipophilic tetracosane chains and water), that all molecules from the beginning adsorb in the more compressed state (equivalent to the compressed state for ACE-10 and ACE-16). The expanded state is thus favorable only for not-too-hydrophobic ACEs. In other words, a proper balance between the hydrophilic and hydrophobic parts of the surfactant must be maintained to maximize the surface activity of the expanded state.

To better address the question of the structure of the adsorbed layer of ACE molecules, X-ray (XR) and neutron reflectivity (NR) studies of ACE-16 and ACE-24 adsorbed at liquid−liquid interface may provide additional information.[25,26] Using XR, the long-chain ACE-24 has been shown to form a dense monolayer at the hexane−water interface with an estimated thickness of about 29 Å, and an average area per molecule of 60 Å^2. The XR experiment allowed to distinguish two parts of the densely packed layer: a more rigid headgroup region together with a few closest methylene units, and a more disordered remainder of the alkyl chains. The first part is tilted with respect to the interfacial normal by ca. 40° and contains some water and hexane intermixed, while the second, less ordered, besides the alkyl chains of ACE-24, contains some hexane molecules from the bulk organic phase. The picture provided by the XR data for ACE-24 is schematically drawn in Figure 5 (right panel).

However, the ACE-16 adsorbed layer, as probed by NR, is much more diffuse and consists of two distinguishable layers of adsorbed molecules stretching across both sides of the hexadecane−water interface. The oil-side part of the monolayer extends up to 17 Å, which would correspond to the part of the hexadecyl chains furthest from the headgroup of ACE-16. The

dx.doi.org/10.1021/jp3017985 | J. Phys. Chem. C 2012, 116, 12584−12590

remainder of the adsorbed layer extends into the aqueous phase. However, the large thickness of this aqueous part of the adsorbed layer (38 Å) suggests that it must comprise also some loosely adsorbed ACE-16 molecules.[25]

The differences between short- and long-chain ACEs observed in interfacial tension behavior at the toluene−water interface described in this article are fully consistent with the structural differences concluded from the earlier XR and NR studies. This prompted us to assign the two modes of adsorption for ACE-16 (and probably also for ACE-10, although no X-ray or neutron reflectivity data is available for this short-chain ACE) to two different locations of the adsorbed ACE molecules in the interfacial region. The loosely packed state with high area per molecule (expanded state) would correspond to the molecules loosely adsorbed on the aqueous side of the interface. The ACE molecules in this region experience probably a mixed organic−water environment and occupy a large area, proportional to the overall area of the expanded molecules. The compressed state, however, would correspond to a more classical adsorption site, located in-plane of the interface, resembling these typically described for water−air interfaces. The dense packing of the molecules in this region (similar to that in Langmuir monolayers[25]) results in very small values of area per molecule obtained from the current interfacial tension data. For the molecules with too low a solubility in the mixed organic-aqueous region of the interphase (e.g., ACE-24), the dense packing at the interface (Langmuir-like) remains the only available mode of adsorption. Only molecules with certain solubility in the mixed aqueous−organic interfacial region have a choice between the expanded adsorption sites, forming a loose layer on the aqueous side, and the compressed, low-area-per-molecule sites at the actual interface (Gibbs-like). This feature is generic to most oil−water interfaces, due to their intrinsic diffuse nature, and similar behavior has been observed already in a number of studies.[27−30] In contrast, it is not usually observed at air−water interfaces, which are sharper on a molecular scale, with little intermixing of the two bulk phases. Spontaneously adsorbed (Gibbs) monolayers even at air−water interfaces are usually dense, with adsorbed molecules located in the surface plane.[31] With decreasing solubility of the surfactant in the second liquid phase (aqueous in the present case), the structure of the adsorbed (Gibbs) layers at oil−water interfaces approaches that of insoluble (Langmuir) monolayers. This explains why the ACE-24 isotherm, in contrast to these of ACE-10 and ACE-16, fits well to a simple Langmuir model with only one type of surface adsorption sites.

The dynamic interfacial tension curves for the short-chain ACE derivatives (ACE-10 and ACE-16), in addition to slow nondiffusion controlled decay, display characteristic inflection points, especially pronounced for ACE-16. For *n*-dodecanol and *n*-dodecanoic acid monolayers, a similar behavior has been interpreted as an indication of a phase transition in the adsorbed layer.[32,33] In the case of alkylated azacrown ethers, one could imagine a similar transition between different orientations (expanded and compressed states) of adsorbed ACE molecules as the origin of the inflections in $\gamma(t)$ curves. The fact that the two regimes are so clearly pronounced reflects the significant differences observed in surface activity of the two states for both short-chain ACE molecules. However, the interfacial tension decays remain slow even for ACE-24, where no indication of reorientation was found. Besides, reorientation itself is not expected to be so slow for molecules of the size of ACE used in this study. Therefore, the overall slow kinetics cannot be due to reorientation but rather to other slow process accompanying adsorption. These are most likely related to protonation of the nitrogen atoms of ACE, which would lead to formation of quaternary ammonium salts. Each nitrogen atom in the alkylated ACE molecule is substituted with two alkoxy groups of the crown moiety and one alkyl group of the *n*-alkyl substituent ($C_{10}H_{21}-$, $C_{16}H_{33}-$, or $C_{24}H_{49}-$). The remaining free electron pair can then be used to coordinate cations, e.g., H_3O^+ or metal ions, although our previous kinetic study[21] clearly showed that hydronium ions are the most effective in accelerating the interfacial tension decays, hence probably also have the highest affinity to ACE. The ion-binding ability of ACEs is a central feature that determines their usefulness as ion-carriers in extraction-based systems, like PLM. If, for any reason, the ion-complexation reaction is slow (e.g., slow supply of any of the reagents to the interface), then the overall adsorption kinetics could also be slow. The slow kinetics of adsorption at the interface between toluene and pure water might stem in fact from the low concentration of hydronium ions, typically in Milli-Q water $c_{H3O+} = 10^{-5.5}$ M. The rate of interfacial tension decays is then probably limited by diffusion of both H_3O^+ and ACE toward the interface. Decreasing pH of the aqueous phase provides more and more hydronium ions, facilitating formation of the fast adsorbing protonated ACE. Interestingly, this protonation renders ACE molecules positively charged (a tertiary amine is transformed into a quaternary ammonium cation), hence should increase an electrostatic adsorption barrier. However, this barrier has apparently minor effect on the overall kinetics of adsorption.

■ CONCLUSIONS

Kinetics and thermodynamics of adsorption of three alkylated diazacrown ethers (ACE-10, ACE-16, and ACE-24, with two decyl, hexadecyl, and tetracosane groups attached to the diaza-18-crown-6 moiety) were studied by the drop-shape analysis method. Adsorption of all three derivatives at the toluene−water interface is much slower than expected from the diffusion control. The short-chain derivatives (ACE-10 and ACE-16) display two kinetic regimes in the dynamic interfacial tension decays, which can be assigned to adsorption on the two surface sites corresponding to the expanded and compressed states in the reorientation model. Since for ACE-24 still slow kinetics persists, despite the lack of the transition between the two adsorbed states, one can speculate that the adsorption in the densely packed mode (corresponding to the compressed state for ACE-10 and ACE-16, as well as the only available adsorption state for ACE-24) is the slowest step in the overall adsorption of ACE at the liquid−liquid interface. This step is only weakly dependent on the length of the alkyl chains and involves probably some interfacial reaction of the azacrown ether moiety with hydronium ions from the aqueous phase.

In line with the dynamic interfacial tension observations, the longest alkyl chain derivative (ACE-24) differs significantly from the other two ACEs also in its equilibrium behavior. While the interfacial tension isotherms for the two short-chain derivatives could be described by the reorientation model, the adsorbed layer of ACE-24 is best described by a simple Langmuir model. Interestingly, the area per molecule in the ACE-24 monolayer is very small (43 Å) and the same as that for ACE-10 and ACE-16 in the high surface pressure (compressed) state. In the low surface pressure (expanded) states of the short-chain derivatives, the values of area per

molecule in the adsorbed layers are much higher (322 Å and 525 Å) and reflect the footprints of both the azacrown ether moiety, and their respective alkyl groups. These results, combined with the previous neutron and X-ray reflectivity studies, clearly show that the alkylated azacrown ethers are able to form both loose (Gibbs-like) and dense (Langmuir-like) adsorbed layers at liquid−liquid interfaces, depending on the length of their alkyl groups. Despite an apparent cmc, the ACE molecules probably do not form classical reverse micelles at high concentrations, but this question will be discussed in a separate report.

AUTHOR INFORMATION

Corresponding Author

*E-mail: kamil.wojciechowski@ch.pw.edu.pl.

Present Address

[†]Institute of Physical Chemistry of the Polish Academy of Sciences, 01-224 Warsaw, Poland.

Notes

The authors declare no competing financial interest.

ACKNOWLEDGMENTS

This work was financially supported by the Warsaw University of Technology. Ms Joanna Ciszewska is acknowledged for help in interfacial tension measurements.

REFERENCES

(1) Bradshaw, J. S.; Izatt, R. M. *Acc. Chem. Res.* **1997**, *30*, 338−345.
(2) Elias, H. *Coord. Chem. Rev.* **1999**, *187*, 37−73.
(3) Izatt, R. M.; Pawlak, K.; Bradshaw, J. S.; Bruening, R. L. *Chem. Rev.* **1991**, *91*, 1721−1785.
(4) Zhang, Z.; Buffle, J.; Van Leeuwen, H. P.; Wojciechowski, K. *Anal. Chem.* **2006**, *78*, 5693−5703.
(5) Freiser, H. *Chem. Rev.* **1988**, *88*, 611−616.
(6) Wojciechowski, K.; Kucharek, M.; Buffle, J. *J. Membr. Sci.* **2008**, *314*, 152−162.
(7) Gatto, V. J.; Arnold, K. A.; Viscariello, A. M.; Miller, S. R.; Morgan, C. R.; Gokel, G. W. *J. Org. Chem.* **1986**, *51*, 5373−5384.
(8) Fainerman, V. B.; Makievski, A. V.; Miller, R. *Colloids Surf., A* **1994**, *87*, 61−75.
(9) IsoFit. http://www.thomascat.info/thomascat/Scientific/AdSo/AdSo.htm.
(10) WardTordai. http://www.thomascat.info/thomascat/Scientific/AdSo/AdSo.htm.
(11) Fainerman, V. B.; Lucassen-Reynders, E. H.; Miller, R. *Colloids Surf., A* **1998**, *143*, 141−165.
(12) Makievski, A. V.; Fainerman, V. B.; Bree, M.; Wuestneck, R.; Kraegel, J.; Miller, R. *J. Phys. Chem. B* **1998**, *102*, 417−425.
(13) Joos, P.; Serrien, G. *J. Colloid Interface Sci.* **1991**, *145*, 291−294.
(14) Fainerman, V. B.; Miller, R.; Aksenenko, E. V.; Makievski, A. V.; Kragel, J.; Loglio, G.; Liggieri, L. *Adv. Colloid Interface Sci.* **2000**, *86*, 83−101.
(15) Liggieri, L.; Ferrari, M.; Massa, A.; Ravera, F. *Colloids Surf., A* **1999**, *156*, 455−463.
(16) Miller, R.; Aksenenko, E. V.; Liggieri, L.; Ravera, F.; Ferrari, M.; Fainerman, V. B. *Langmuir* **1999**, *15*, 1328−1336.
(17) Fainerman, V. B.; Miller, R.; Aksenenko, E. V. *Langmuir* **2000**, *16*, 4196−4201.
(18) Fainerman, V. B.; Miller, R.; Moehwald, H. *J. Phys. Chem. B* **2002**, *106*, 809−819.
(19) Fainerman, V. B.; Zholob, S. A.; Lucassen-Reynders, E. H.; Miller, R. *J. Colloid Interface Sci.* **2003**, *261*, 180−183.
(20) Miller, R.; Fainerman, V. B.; Moehwald, H. *J. Colloid Interface Sci.* **2002**, *247*, 193−199.
(21) Wojciechowski, K.; Buffle, J.; Miller, R. *Colloids Surf., A* **2007**, *298*, 63−71.
(22) Wojciechowski, K.; Buffle, J.; Miller, R. *Colloids Surf., A* **2005**, *261*, 49−55.
(23) Israelachvili, J. *Intermolecular and Surface Forces*, 2nd ed.; Academic Press: New York, 2000.
(24) De Wall, S. L.; Barbour, L. J.; Gokel, G. W. *J. Phys. Org. Chem.* **2001**, *14*, 383−391.
(25) Zarbakhsh, A.; Webster, J. R. P.; Wojciechowski, K. *Langmuir* **2009**, *25*, 11569−11575.
(26) Wojciechowski, K.; Gutberlet, T.; Tikhonov, A.; Kashimoto, K.; Schlossman, M. *Chem. Phys. Lett.* **2010**, *487*, 62−66.
(27) Zarbakhsh, A.; Querol, A.; Bowers, J.; Webster, J. R. P. *Faraday Discuss.* **2005**, *129*, 155−167.
(28) Zarbakhsh, A.; Querol, A.; Bowers, J.; Yaseen, M.; Lu, J. R.; Webster, J. R. P. *Langmuir* **2005**, *21*, 11704−11709.
(29) Lu, J. R.; Thomas, R. K.; Binks, B. P.; Fletcher, P. D. I.; Penfold, J. *J. Phys. Chem.* **1995**, *99*, 4113−4123.
(30) Lu, J. R.; Fragneto, G.; Thomas, R. K.; Binks, B. P.; Fletcher, P. D. I.; Penfold, J. *Colloids Surf., A* **1998**, *135*, 277−281.
(31) Lu, J. R.; Hromadova, M.; Simister, E. A.; Thomas, R. K.; Penfold, J. *J. Phys. Chem.* **1994**, *98*, 11519−11526.
(32) Tsay, R.; Tsai, H.; Wu, T.; Lin, S. *Colloids Surf., A* **2010**, *369*, 148−153.
(33) Prosser, A. J.; Retter, U.; Lunkenheimer, K. *Langmuir* **2004**, *20*, 2720−2725.